Journal of the Australian Ceramic Society
https://doi.org/10.1007/s41779-024-01064-0

RESEARCH

Plant-mediated green route to the synthesis of zinc oxide nanoparticles: in vitro antibacterial potential

Deniz Kadir Takcı[1] · Melis Sumengen Ozdenefe[2] · Tahsin Huner[3] · Hatice Aysun Mercimek Takcı[4]

Received: 24 April 2024 / Revised: 14 June 2024 / Accepted: 8 July 2024

Abstract

The plant-mediated, sustainable, facile, eco-friendly, and simple green approaches for the fabrication of metal oxide nanoparticles (NPs) have recently attracted the ever-increasing attention of the scientific community. To date, there has not been any research on green synthesis of ZnO-NPs by *Piper guineense* (Uziza) seeds widely used as a therapeutic agent is the novelty of the current study. The bioaugmented ZnO-NPs have been manufactured by Uziza seed extract using zinc acetate dihydrate as the precursor and sodium hydroxide with calcination. The hexagonal/spherical crystalline structure at high purely with a mean size of 7.39 nm was confirmed via XRD and SEM analyses of ZnO-NPs. A strong absorption peak at about 350 nm, specific for ZnO-NPs, was observed by a UV-visible spectrometer. The optical bandgap of ZnO-NPs was estimated as about 3.58 eV by the Kubelka-Munk formula. FTIR findings indicated the presence of biofunctional groups responsible for the bioreduction of bulk zinc acetate to ZnO-NPs. The growth rates of *E. coli* (ATCC 25,922) significantly decreased with ZnO-NPs exhibited compared to the controls. This is making ZnO-NPs promising effective candidates for medical sectors and environmental applications. This current study is hoped to supply a better understanding of the phytosynthesis of ZnO-NPs and promote the advance of green approaches based on plants.

Keywords Antibacterial · Green synthesis · Nanoparticles · *P. guineense* · ZnO

Introduction

Nanotechnology studies its history dating back to 1959, are now accepted as a modern and revolutionary technology having numerous branches proven in industrial fields [1, 2]. The state-of-the-art advances in nanotechnology are many nanoscale device developments showing unexpected popularity in several scientific fields such as biomedicine, environmental and material science, electronics, computing, and optics [3–7]. Nanoparticles have unique physical characteristics that are interrelated and exhibit significant distinction from bulk materials: the high mobility in the free state, the high surface area-to-volume ratio, and the quantum effects [8]. Nanoparticle dimensions are defined in the range of 1–100 nm and can be classified into their shape, size, and material features. Metallic nanoparticles among these nanostructures possess advanced properties including quantum confinement, optical, plasmon excitation, and large surface energies [9].

Zinc oxide (ZnO) possessing visible transparency (wide optical bandgap, Eg = 3.37 eV) and high electrical conductivity (large exciton binding energy of 60 meV) is an II-VI semiconducting ceramic material [10, 11]. In particular, it has some characteristic features such as inexpensive, biocompatible, non-toxic, high electron mobility, great chemical, and thermal stability, high optical transmittance as well as it is fabricated easily [12, 13]. Because of its properties mentioned above and being the most abundant metal oxide after iron, ZnO is one of the most researched nanomaterials [14]. Due to the uncomplicated control of ZnO properties, ZnO-NPs with various sizes and shapes (flower-like

✉ Deniz Kadir Takcı
dktakci@gmail.com

1 Vocational High School of Health Services, Opticianry Program, Kilis 7 Aralik University, Kilis 79000, Türkiye

2 Department of Biomedical Engineering, Near East University, North Cyprus via Mersin 10, Nicosia, Türkiye

3 Institute of Science and Technology, Kilis 7 Aralik University, Kilis 79000, Türkiye

4 Department of Molecular Biology and Genetics, Kilis 7 Aralik University, Kilis 79000, Türkiye

Published online: 30 July 2024

nanostructures, nanowires, nanotubes, nanobelts, nanorings, and nanorods) can be synthesized [15].

ZnO-NPs might be prepared using many synthesis approaches (chemical, physical, and biological) by manipulating the fabrication mechanisms [16]. Nowadays, material scientists are focused on costless effective, simple, nontoxic, and eco-friendly methods for the synthesizing of nanoscale materials [17]. Thus, chemical and physical synthesis strategies have been gradually replaced by biological or "green" methods due to disadvantages such as the release of toxic and harmful chemicals, the requirement of complex and expensive equipment, the necessity of high pressure and temperature, and the consumption of a large amount of energy [18].

Here, we discuss the plant-based green synthesis of ZnO-NPs using the aqueous extracts of *Piper guineense* (Uziza) seeds, in Nigeria. The green synthesized ZnO-NPs will be characterized by modern techniques such as scanning electron microscopy (SEM), energy dispersive X-ray analysis (EDAX), ultraviolet (UV-visible) spectroscopy, Fourier transform infrared (FTIR) spectroscopy, and X-ray diffraction (XRD). Besides, the antimicrobial potential of *E.coli* ATCC 25,922 strain of ZnO-NPs will be exhibited.

Materials and methods

Preparation of seed extract

The dried seeds of *P. guineense* (Uziza) (Fig. 1(a) were purchased from the Ibusa local market in Delta State, Nigeria, in 2023. Seeds (Fig. 1(b) were firstly washed using distilled water, dried in the sunlight, and then powdered crushing by the electric blender. The powdered seeds (2 g) were soaked in 100 mL distilled for 15 min at 60 °C temperature. After cooling down, the obtained suspension was filtered through a Whatman No.1 filter paper. This seed extract was kept at +4 °C till used as a reducing and stabilizing agent for NP synthesis [19].

Green synthesis of ZnO-NPs

0.25 g of $Zn(CH_3COO)_2.2H_2O$ was dissolved in 25 mL of seed extract under continuous stirring until a homogeneous mixture for synthesizing ZnO-NPs by green approach. Then, this mixture was heated on a magnetic stirrer at 60 C for 2 h. Following allowed to cool down at 25 °C, the pH of the solution was adjusted to 10 using 2 M NaOH. The solution color of the initially transparent was turned to slightly yellow and finally milky white, indicating the formation of ZnO-NPs. The obtained reaction mixture was centrifuged at 5.000 rpm for 20 min. and the supernatant was discarded. Finally, the remaining pellet was washed three times with distilled water and absolute ethanol and dried in air at room temperature for 3 h. For the yielding of nanomaterial powder products, ZnO-NPs were calcined at 500 °C for 2 h in a muffle furnace to remove any impurities [2]. Thus, ZnO-NPs were obtained and labeled for further physical characterizations and antibacterial analysis. The green synthesis of ZnO-NPs is schematized in Fig. 2.

Characterization of ZnO-NPs

The physicochemical properties of ZnO-NPs were investigated using different characterization techniques. The elemental composition and surface morphology of ZnO-NPs were inspected using a field emission scanning electron microscope (FESEM, FEI Quanta-FEG-6250) with energy dispersive X-ray analysis (EDX) at 20 kV voltage. The vibrational bands related to the functional group composition of ZnO-NPs were analyzed by a Fourier transform infrared (FTIR) spectrometer (Jasco FT/IR-6700 Spectrophotometer) in the range of 4000–400 cm^{-1}. The crystalline nature of ZnO-NPs nanoparticles was exhibited by a Panalytical Empyrean XRD diffractometer Cu Kα radiation (λ = 1.54059 Å) radiation obtained at 45 kV and 40 mA, 10◦ to 90◦ with 0.01◦ step size. The diffuse reflectance spectra of ZnO-NPs were measured using an Ultraviolet-visible spectrophotometer (SHIMADZU UV-3600 PLUS).

Fig. 1 (**a**) *P. guineense* (Uziza) plant (**b**) Seeds of Uziza

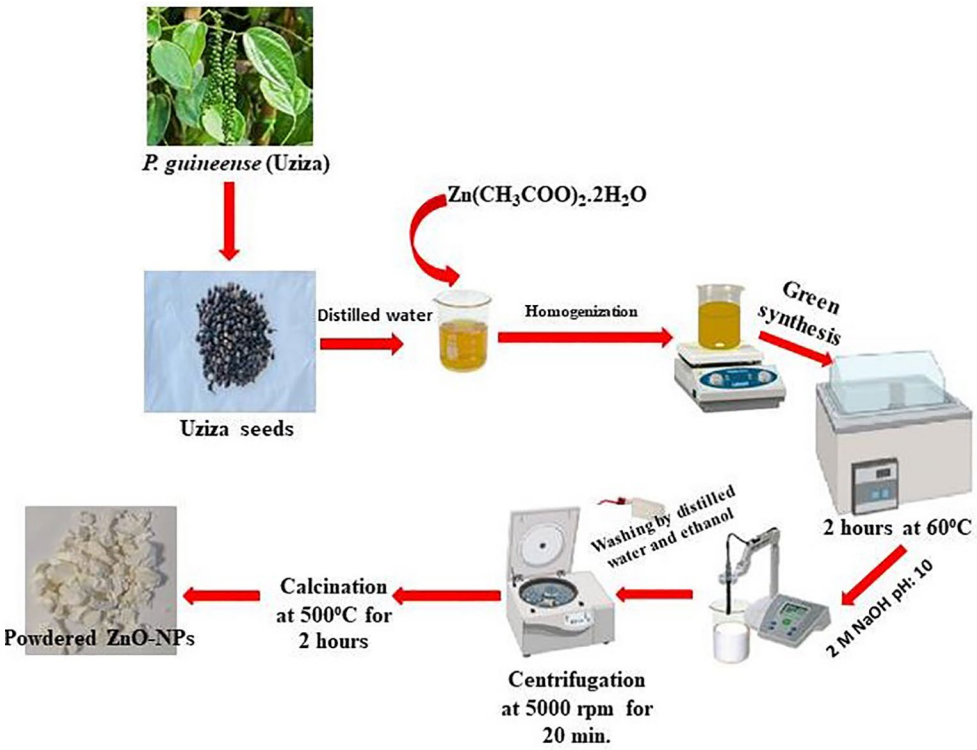

Fig. 2 Fabrication scheme of ZnO-NPs using Uziza seeds

Antibacterial assay on *Escherichia coli*

Bacterial stock cultures of *E. coli* (ATCC 25,922) were acquired from 80 °C freezer stocks including 30% glycerol. 100 µL of stock solution is transferred into 5 mL of Luria Broth, placed on a shaker (180 rpm), and then incubated for 24 h at 37 °C. The overnight culture of strain was streaked onto Nutrient Agar using a sterile loop and incubated for 12–24 h at 37 °C. Following incubation, a single colony of strain was selected and stocked into the sterile Nutrient Agar for further in vitro anti-bacterial assay.

The antibacterial effect of ZnO-NPs on *E. coli* was estimated by counting viable bacterial cell concentrations before and after exposure to the NPs. Briefly, the density of the overnight bacterial culture growth in Luria Broth was adjusted to 0.5 on the McFarland scale by saline (0.9% NaCl). 100 µL of this bacterial suspension was inoculated into Luria broth including 25, 50, and 100 µg/mL ZnO-NPs, and incubated at 37 °C for 12 h. Then, an amount of 100 µL of fresh suspension was spread over the surface of Plate Count Agar in triplicate, and plates were incubated at 37 °C for 12–24 h, and colony forming units/milliliter (CFU/mL) were counted. Results were calculated using the equation:

Equation: Cfu(c)-Cfu(s)/Cfu(c)*100.

Results and discussion

P. guineense Schumach & Thonn, also called "West African black pepper, Guinea cubeb, Benin pepper, and Ashanti pepper, has high nutritional qualities, vitamins, and minerals [20]. It is a culinary spice thriving as native to the tropical rain forest of Africa and also partly cultivated in Southern Nigeria [21]. Due to its remarkable biological activities such as managing anemia, bronchitis, cancer, carminative, cough, rheumatism, and stomach ache, it is widely used as a traditional source of medicine [22, 23]. It is usually named Uziza and Iyre in the South-Eastern Nigerian and Yoruba, respectively [24]. In addition, numerous phytochemicals, the constituents of crude protein, dry matter, crude fiber, crude lipid, high mineral elements, carbohydrates, and ash were also reported in the dry biomass of Uziza seeds [24, 25]. This major substance in Uziza seed biomass is assumed to contribute to the green synthesis of biomedically significant ZnO-NPs.

The fabrication of biogenic ZnO-NPs was performed using aqueous seed extracts of Uziza as reducing, capping, and stabilizing agents. Following the addition of NaOH into the mixture involving $Zn(CH_3COO)_2.2H_2O$ precursor and plant extract, the formation of milky white precipitate was confirmed to be the plant-mediated photosynthesis of ZnO-NPs. The fine white powder obtained subsequently from the washing, drying, and calcination steps was labeled as ZnO-NPs.

The toxic-free substances in Uziza seed extract can be asserted to act as reducing agents that converted the metal precursor to ZnO-NPs. This finding related to phytofabrication was supported by the literature studies revealing the biosynthesis of ZnO-NPs mainly depends on the species of plant used [26, 27].

These phytochemical agents are found at different concentrations depending on plant types and have a significant effect on the synthesis, stabilization, and quantity of ZnO-NPs. The bio-reduction mechanism of ZnO-NPs mediated phytochemicals is examined by three main strategies: (1) the activation phase: the bounding of the zinc ions in salt solutions to the reducing metabolites presented in Uziza seed extract, then the reduction of metal ions, and the nucleation of metal atoms. (2) the growth phase referring to Ostwald ripening: Increase in the thermodynamic stability of ZnO-NPs as a result of the coalescing of nearby small NPs spontaneously into larger particles. (3) termination phase: the oxidizing resulting in the linking of metal ions, and the determining of the final shape [28].

A strong absorption peak of around 350 nm showed the successful synthesis of ZnO NPs via the green approach. This result satisfies the characteristic ZnO absorption peak due to tending to have shorter wavelengths of nanoscale materials [29, 30]. The optical bandgap of NPs was estimated by a graph plotted (F(R)hv)2 versus photon energy (hv) in Fig. 3's inset. For a given wavelength the Kubelka-Munk formula adapts the diffuse reflectance data to the function F (R),

$$F(R) = \frac{K}{S} = \frac{(1-R)^2}{2R} \tag{1}$$

where k is the absorption coefficient, R_∞ is the diffuse reflectance, and s is the scattering coefficient. The indirect

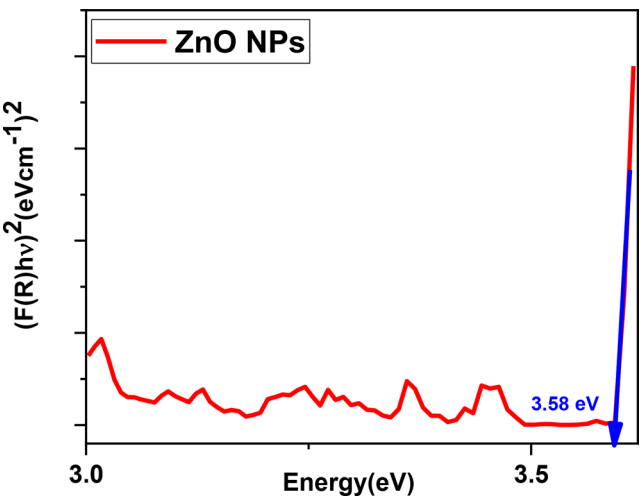

Fig. 3 (F(R)hv)2 versus photon energy (hv) spectrum of ZnO-NPs

bandgap of ZnO-NPs was estimated by extrapolation of the linear portion of the (F(R) = 0) curve to the x-axis obtained as 3.58 eV, depending on the sizes of ZnO-NPs. The optical bandgap value agrees with the literature [31, 32]. The bandgap of NPs varies depending on various structural factors involving oxygen deficiency, grain size, lattice strain, and surface roughness [33]. The greater our bandgap value than the bulk ZnO (3.37 eV) may be explained by the small crystallite sizes of photosynthesized NPs.

The green synthesis of ZnO-NPs mediated Uziza seed extract was displayed by a FE-SEM examination. The size, size distribution, and shape of ZnO-NPs are shown in Fig. 4(a). The SEM images recorded at a magnification of 10.000x, 50.000x, and 100.000x display that the biosynthesized ZnO-NPs are mostly spherical and well-dispersed without any aggregation. The selected area EDX pattern demonstrates the element compositions of nanoparticles with an average size of 7.39 nm in Fig. 4(b). The particle shape and size expressed by the SEM were further confirmed using XRD. The shape and size of biogenic ZnO-NPs are closely matched with the values previously reported [34]. The size and shape of ZnO-NPs play an important role in the antibacterial activity against pathogens. NPs with low size (4.27 nm) and spherical shape tend to penetrate easily into the bacterial cell wall. This is an enormous capability in treating clinical infectious bacterial strains. The purity of synthesized ZnO-NPs and the presence of Zinc in its oxide form were certified by EDX analysis. The strong emission peaks of Zn at ~1 keV, 8.6 keV, and 9.5 keV, and the emission peaks belonging to carbon at ~0.25 keV and oxygen at ~0.5 keV indicated the successful photo-synthesis of ZnO-NPs. The elemental composition of the ZnO-NP revealing 69.38% zinc, 25.12% oxygen, and 5.51% carbon are consistent with the weight peaks that were determined earlier [35, 36].

The XRD pattern of biosynthesized ZnO-NP mediated Uziza is illustrated by the definite line broadening of the characteristic peaks in Fig. 5. These Bragg diffraction peaks with 2θ values associated ZnO-NPs identified as 31.9°, 34.6°, 36.4°, and 56.7°, indexed to the (100), (002), (101), and (110) lattice planes, respectively. These peaks matching well with the standard card (JCPDS Card No. 98-002-9272) confirmed the spherical to the hexagonal phase of ZnO-NPs with space group P 63 mc. The absence of any distinctive XRD peaks apart from the sharp ZnO peaks indicates the purity and high crystallinity structure of NPs. These peaks are paralleled to those of previous studies [37, 38]. The average crystalline size (D) of fabricated ZnO-NPs calculated from the most intense peaks using Debye-Scherrer's equation:

$$D = \frac{k\lambda}{\beta_{hkl} cos\theta} \tag{2}$$

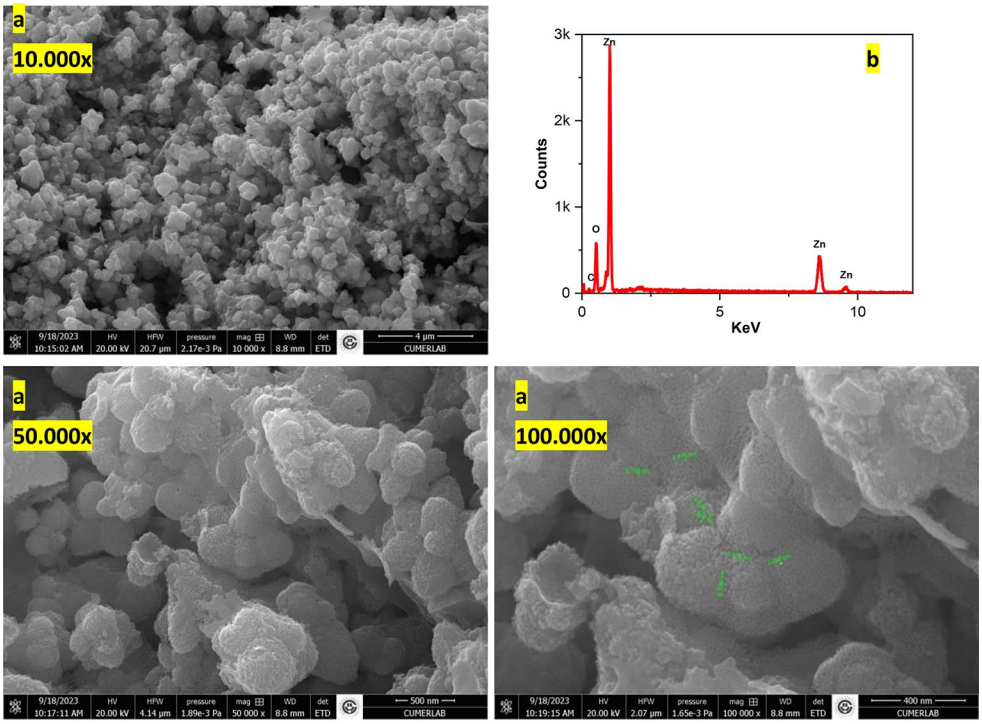

Fig. 4 (**a**) SEM images of ZnO-NPs at different magnifications and (**b**) elemental composition of ZnO-NPs

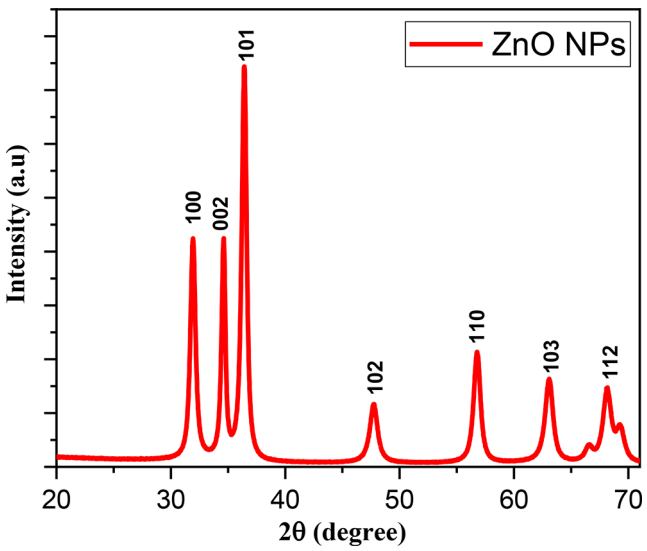

Fig. 5 Typical XRD pattern of biogenic ZnO-NPs

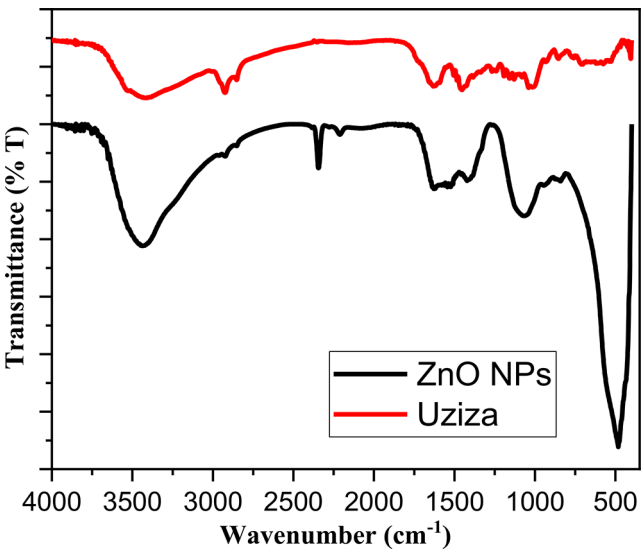

Fig. 6 FTIR spectrum of ZnO-NPs and Uziza

where λ is the X-ray wavelength (1.5406), k 0.94 is Scherrer's constant, θ is the FWHM in radians of the peak, and β is the Bragg diffraction angle [39]. D value depicted from the highest intensity peak corresponding to 101 planes located at position 36.4° is in ranges from 10 nm. The crystalline size of ZnO-NPs detected by Scherrer's equation is by those of SEM images.

As shown in Fig. 6, the functional groups in the Uziza extract and ZnO-NPs were classified by FT-IR analysis. To demonstrate the organic substances (phenolics and flavonoids) still kept in a structure after the calcination step performed throughout the manufacture of ZnO, the FTIR spectrum of aqueous extract and NPs were compared in Table 1. Broad absorption peaks at 3435.77 and 3421.62 cm^{-1} in a higher energy region are related to the -OH stretching frequency of phenolic and flavonoid components. The absorption bands at 2922.97 and 2924.78 cm^{-1} are characteristic of the–C-H-in alkanes N–H or the C=O stretching vibrations, respectively. The following bands at around 1630.66–1627.20 cm^{-1} correspond to C=O stretching carboxylic vibration in the amide I and amide II groups. C-H stretching vibrations of the aromatic ring are attributed to the bands (1452.48 and 1422.99 cm^{-1}).

Table 1 The absorption spectra of probable assigned phytochemical compounds by FTIR

Possible assignment	Absorption peaks in Uziza (cm^{-1})	Absorption peaks in ZnO-NPs (cm^{-1})
-OH stretching	3421.62	3435.77
–C-H stretching in alkanes	2924.78	2922.97
C = O stretching in carboxylic groups	1630.66	1627.20
–CH stretching in aromatic rings	1452.48	1422.99
C-N stretching in aliphatic amines	1012.93	1056.53
C = C bending in alkene	850.98	844.32
ZnO		482.34

The sharp bands at 1012.93 and 1056.53 cm^{-1} are due to the–C-N stretching vibrations of aliphatic amines. The other bands at 850.98–844.32 cm^{-1} are corresponding to the C-H bending of carboxylic acids and aromatics. The spectral peak at 482.34 cm^{-1} corresponded to Zn and O bonding vibrations confirming behaved as a reducing and capping agent phenolic compounds for the synthesized ZnO-NPs. These FT-IR results related to the roles of flavonoids, protein molecules, and the other functional groups in the bioreduction of metal ions were supported by previous findings [40, 41]. Our peak regarding the characteristic stretching vibration band of Zn-O at wavelength 469 cm^{-1} is in accordance with those of literature findings at 400 to 500 cm^{-1} [42], 450 cm^{-1}, and 600 cm^{-1} [35], and 486 cm^{-1} [43].

Table 2 The colonies number on the PCA plates of *E. coli* (ATCC 25,922) cells grown with various concentrations of ZnO-NPs, plant extract, and without ZnO-NPs

E. coli growth conditions	Number of bacterial colonies (CFU/mL)	% Inhibition
without ZnO-NPs	$91.00\times10^{8}\pm3.50$	%0.00
with Uziza extract	$672\times10^{7}\pm15.00$	%26.15
with 25 µg/mL ZnO-NPs	$335\times10^{2}\pm10.00$	%99.99
with 50 µg /mL ZnO-NPs	$88\times10^{2}\pm9.00$	%99.99
with 100 µg/mL ZnO-NPs	$46\times10^{2}\pm6.00$	%99.99

The antibacterial efficacy of biogenic ZnO-NPs was scrutinized by counting total viable cells as observed in Fig. 7. % Inhibition and total viable count (CFU) in cultures exposed to ZnO-NPs at various concentrations are summarized in Table 2. The strong inhibitory effect of ZnO-NPs on *E. coli* growth was noted as compared to the control samples without NPs. The highest bactericidal activity was notified as 99.99% in comparison with control (0.0%) regardless of ZnO-NPs concentrations. Our results agree with those of Awwad et al. (2020); Iqbal et al. (2021); Ahmad et al. (2022); Vo et al. (2023) [44–47]. The excellent antibacterial efficiency of ZnO-NPs synthesized via

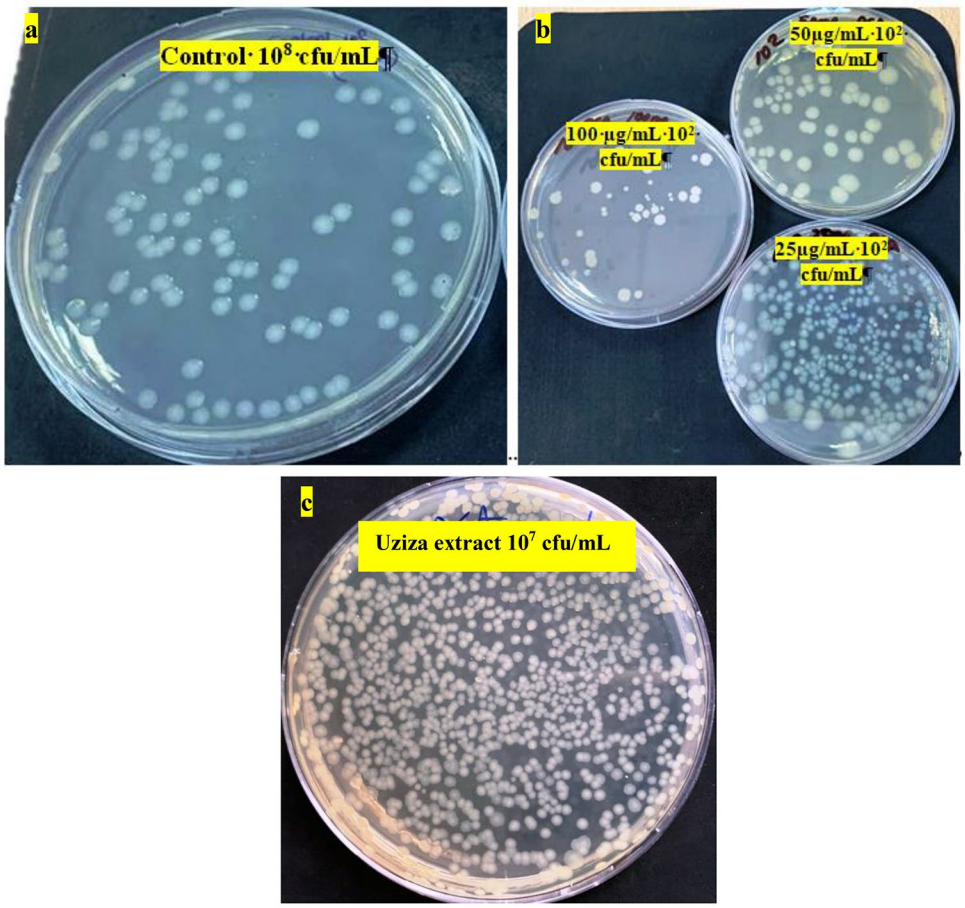

Fig. 7 The viability of *E.coli* (ATCC 25,922) cells (**a**) without ZnO-NPs and (**b**) with ZnO-NPs at 25, 50, and 100 µg/mL and (**c**) with Uziza extract

the green route depends on having a larger surface area of NPs with smaller sizes and showing one of the possible inhibition mechanisms mentioned in the literature. Antibacterial actions of ZnO-NPs involve (1) the generation of reactive oxygen species (ROS) causing oxidative stress, damage of DNA, and disruption of cell membrane and finally leading to cell lysis; (2) the destroying of the cellular integrity and eventually bacterial cell death by the interaction of ZnO-NPs with bacterial cell membrane, cytoplasm, DNA, RNA, and protein; (3) the direct electrostatic interactions between the bacterial cell wall and ZnO-NPs and the accumulations in the lipid layer resulting in the disruption of plasma membrane and leaking of intracellular components [48–50].

Conclusions

Here, we imply a facile, simple, and one-pot eco-friendly green synthesis of biobased ZnO-NPs by *P. guineense* extract. This current study demonstrated the successful synthesis of hexagonal/spherical ZnO-NPs by reducing, capping, and stabilizing agents indicating the presence of phytochemical compounds in the extract. To the best of our knowledge, this study is the first to research the phytosynthesis of ZnO-NPs by *P. guineense* from Nigeria. The strong inhibitory ability for biogenic ZnO-NPs on *E. coli* strain showing high resistance against standard antibiotics is considered to help the developed novel antimicrobial agents to alternative the costly and less efficient drugs that are used in the clinical setup. We hope that our data tenders to the readers to the promising ideas to find out original and up-to-date strategies for metal NPs that can be used in biological systems-related applications.

Acknowledgements We thank Harvest Ndubisi Onwordi for providing the *Piper guineense* (Uziza) plant.

Funding Open access funding provided by the Scientific and Technological Research Council of Türkiye (TÜBİTAK).

Data availability The datasets generated during and/or analysed during the currentstudy are available from the corresponding author on reasonable request.

Declarations

Competing interests The authors declare that they have no known competing financial interests or personal relationships that could have appeared to influence the work reported in this paper.

References

1. Bokhari, H.: Exploitation of microbial forensics and nanotechnology for the monitoring of emerging pathogens. Crit. Rev. Microbiol. **44**, 504–521 (2018). https://doi.org/10.1080/1040841X.2018.1444013
2. Faisal, S., Jan, H., Shah, S.A., Shah, S., Khan, A., Akbar, M.T., Rizwan, M., Wajidullah, F.J., Akhtar, N., Khattak, A., Syed, S.: Green synthesis of zinc oxide (ZnO) nanoparticles using aqueous fruit extracts of *Myristica fragrans*: Their characterizations and biological and environmental applications. ACS Omega. **6**, 9709–9722 (2021). https://doi.org/10.1021/acsomega.1c00310
3. Shaba, E.Y., Jacob, J.O., Tijani, J.O., Suleiman, M.A.T.: A critical review of synthesis parameters affecting the properties of zinc oxide nanoparticle and its application in wastewater treatment. Appl. Water Sci. **11**, 48 (2021). https://doi.org/10.1007/s13201-021-01370-z
4. Erum, N., Ahmad, J.: Structural, elastic, and mechanical properties of cubic perovskite materials. Arch. Adv. Eng. Sci. **2**(1), 24–29 (2024). https://doi.org/10.47852/bonviewAAES3202944
5. Feng, J., Safaei, B., Qin, Z., Chu, F.: Nature-inspired energy dissipation sandwich composites reinforced with high-friction graphene. Compos. Sci. Technol. **233**, 109925 (2023). https://doi.org/10.1016/j.compscitech.2023.109925
6. Feng, J., Safaei, B., Qin, Z., Chu, F., Scarpa, F.: Bio-inspired metallic cellular material with extraordinary energy dissipation capability. J. Chem. Eng. **475**, 146382 (2023). https://doi.org/10.1016/j.cej.2023.146382
7. Shekoofa, O., Wang, J., Li, D.: Fabrication of N-type nanocrystalline silicon thin film by magnetron sputtering and antimony-induced crystallization. Arch. Adv. Eng. Sci. **2**(2), 71–78 (2024). https://doi.org/10.47852/bonviewAAES32021040
8. Zhou, X.Q., Hayat, Z., Zhang, D.D., Li, M.Y., Hu, S., Wu, Q., Cao, Y.F., Yuan, Y.: Zinc oxide nanoparticles: Synthesis, characterization, modification, and applications in food and agriculture. Processes. **11**, 1193 (2023). https://doi.org/10.3390/pr11041193
9. Thakur, M., Sharma, A., Chandel, M., Pathania, D.: Modern applications and current status of green nanotechnology in environmental industry. In: Shanker, U., Hussain, C.M., Rani, M. (eds.) Green Functionalized Nanomaterials for Environmental Applications, pp. 259–281. Elsevier (2022)
10. Lee, W., Yeop, J., Heo, J., Yoon, Y.J., Park, S.Y., Jeong, J., Shin, Y.S., Kim, J.W., An, N.G., Kim, D.S., Park, J., Kim, J.Y.: High colloidal stability ZnO nanoparticles independent on solvent polarity and their application in polymer solar cells. Sci. Rep. **10**, 18055 (2020). https://doi.org/10.1038/s41598-020-75070-0
11. Sedefoglu, N.: Green synthesis of ZnO nanoparticles by *Myrtus communis* plant extract with investigation of effect of precursor, calcination temperature and study of photocatalytic performance. Ceram. Int. **50**, 9884–9895 (2024). https://doi.org/10.1016/j.ceramint.2024.01.387
12. Mehnath, S., Das, A.K., Verma, S.K., Jeyaraj, M.: Biosynthesized/green-synthesized nanomaterials as potential vehicles for delivery of antibiotics/drugs. In: Verma, S.K., Das, A.K. (eds.) Biosynthesized Nanomaterials, Comprehensive Analytical Chemistry, pp. 363–432. Elsevier (2021)

13. Raj, R., Gupta, H., Purohit, L.P.: Highly transparent and conducting Al-doped ZnO as a promising material for optoelectronic applications. Pramana–J Phys. **95**, 87 (2021). https://doi.org/10.1007/s12043-021-02123-y
14. Ramanathan, S., Gopinath, S.C.B., Arshad, M.K.M., Poopalan, P., Perumal, V.: Nanoparticle synthetic methods: Strength and limitations. In: Gopinath, S.C.B., Gang, F. (eds.) Nanoparticles in Analytical and Medical Devices, pp. 31–43. Elsevier (2021)
15. Chu, D., Masuda, Y., Ohji, T., Kato, K.: Formation and photocatalytic application of ZnO nanotubes using aqueous solution. Langmuir. **26**(4), 2811–2815 (2010). https://doi.org/10.1021/la902866a
16. Rohani, R., Dzulkharnien, N.S.F., Harun, N.H., Ilias, I.A.: Green approaches, potentials, and applications of zinc oxide nanoparticles in surface coatings and films. Bioinorg. Chem. Appl. 3077747 (2022). (2022). https://doi.org/10.1155/2022/3077747
17. Mat'átková, O., Michailidu, J., Miškovská, A., Kolouchová, I., Masák, J., Cejkovˇ, A.: Antimicrobial properties and applications of metal nanoparticles biosynthesized by green methods. Biotechnol. Adv. **58**, 107905 (2022). https://doi.org/10.1016/j.biotechadv.2022.107905
18. Ying, S., Guan, Z., Ofoegbu, P.C., Clubb, P., Rico, C., He, F., Hong, J.: Green synthesis of nanoparticles:Current developments and limitations. Environ. Technol. Innov. **26**, 102336 (2022). https://doi.org/10.1016/j.eti.2022.102336
19. Takci, D.K., Genc, S., Takci, M.: Cinnamon-based rapid biosynthesis of silver nanoparticles; its characterization and antibacterial properties. J. Cryst. Growth. **623**, 127416 (2023). https://doi.org/10.1016/j.jcrysgro.2023.127416
20. Hannah Ademuyiwa, O., Mofoluwaso Fasogbon, B., Ayodeji Adebo, O.: The potential role of *Piper guineense* (black pepper) in managing geriatric brain aging: A review. Crit. Rev. Food Sci. Nutr. **63**, 2840–2850 (2023). https://doi.org/10.1080/10408398.2021.1980764
21. Ameh, S.J., Obodozie, O.O., Inyang, U.S., Abubakar, M.S., Garba, M.: Climbing black pepper (*Piper guineense*) seeds as an antisickling remedy. In: Preedy, V.R., Watson, R.R., Patel, V.B. (eds.) Nuts and Seeds in Health and Disease Prevention, pp. 333–343. Academic (2011)
22. Tamokou, J.D.D., Mbaveng, A.T., Kuete, V.: Antimicrobial activities of African medicinal spices and vegetables. In: Kute, V. (ed.) Medicinal Spices and Vegetables from Africa, Therapeutic Potential against Metabolic, Inflammatory, Infectious and Systemic Diseases, pp. 207–237. Academic (2017)
23. Martins, M., Jerônimo, G.T., Brum, A., Tancredo, K.R., Bertaglia, E.A., Furtado, W., Lehmann, N., Azevedo, P.F.O., Mouriño, J.L.P.: Antiparasitic agents. In: Kibenge, F.S.B., Baldisserotto, B., Chong, R.S.-M. (eds.) Aquaculture Pharmacology, pp. 169–217. Academic, Elsevier (2021)
24. Uzoekwe, N.M., Ezenwajıugo, C.E.: Phytochemicals, elemental and proximate analyses of *Piper Guineense* leaves. J. Appl. Sci. Environ. Manage. **27**, 657–663 (2023). https://doi.org/10.4314/jasem.v27i4.3
25. Imo, C., Yakubu, O.E., Imo, N.G., Udegbunam, I.S., Tatah, S.V., Onukwugha, O.J.: Proximate, mineral and phytochemical composition of *Piper guineense* seeds and leaves. J. Biol. Sci. **18**, 329–337 (2018). https://doi.org/10.3923/jbs.2018.329.337
26. Jayachandran, A., Aswathy, T.R., Achuthsankar, S.N.: Green synthesis and characterization of zinc oxide nanoparticles using *Cayratia pedata* leaf extract. Biochem. Biophys. Rep. **26**, 100995 (2021). https://doi.org/10.1016/j.bbrep.2021.100995
27. Naiel, B., Fawzy, M., Halmy, M.W.A., Mahmoud, A.E.D.: Green synthesis of zinc oxide nanoparticles using sea lavender (*Limonium Pruinosum* L. Chaz.) Extract: Characterization, evaluation of anti–skin cancer, antimicrobial and antioxidant potentials. Sci. Rep. **12**, 20370 (2022). https://doi.org/10.1038/s41598-022-24805-2
28. Abdelbaky, A.S., Mohamed, A.M.H.A., Sharaky, M., Mohamed, N.A., Diab, Y.M.: Green approach for the synthesis of ZnO nanoparticles using *Cymbopogon citratus* aqueous leaf extract: Characterization and evaluation of their biological activities. Chem. Biol. Technol. Agric. **10**, 63 (2023). https://doi.org/10.1186/s40538-023-00432-5
29. Osuntokun, J., Onwudiwe, D.C., Ebenso, E.E.: Green synthesis of ZnO nanoparticles using aqueous *Brassica oleracea* L. var. *Italica* and the photocatalytic activity. Green. Chem. Lett. Rev. **12**, 444–457 (2019). https://doi.org/10.1080/17518253.2019.1687761
30. Meena, P.L., Poswal, K., Surela, A.K.: Facile synthesis of ZnO nanoparticles for the efective photodegradation of malachite green dye in aqueous solution.Water Environ. J. **36**, 25 (2022). https://doi.org/10.1111/wej.12783
31. Onal, M., Altıokka, B.: Optimization of EDTA–Ammonia ratio for chemically deposited layers of ZnO nanoparticles. Crystallogr. Rep. **65**, 1237–1241 (2020). https://doi.org/10.1134/S1063774520070135
32. Ikram, M., Shahid, H., Haider, J., Haider, A., Naz, S., Ul-Hamid, A., Shahzadi, I., Naz, M., Nabgan, W., Ali, S.: Nb/starch-doped ZnO nanostructures for polluted water treatment and antimicrobial applications: Molecular docking analysis. ACS Omega. **7**, 39347–39361 (2022). https://doi.org/10.1021/acsomega.2c05569
33. Wang, F.-H., Chang, C.-L.: Effect of substrate temperature on transparent conducting Al and F co-doped ZnO thin films prepared by rf magnetron sputtering. Appl. Surf. Sci. **370**, 83–91 (2016). https://doi.org/10.1016/j.apsusc.2016.02.161
34. Hassan Basri, H., Talib, R.A., Sukor, R., Othman, S.H., Ariffin, H.: Effect of synthesis temperature on the size of ZnO nanoparticles derived from pineapple peel extract and antibacterial activity of ZnO–starch nanocomposite films. Nanomaterials. **10**, 1061 (2020). https://doi.org/10.3390/nano10061061
35. Fakhari, S., Jamzad, M., Fard, H.K.: Green synthesis of zinc oxide nanoparticles: A comparison. Green. Chem. Lett. Rev. **12**, 19–24 (2019). https://doi.org/10.1080/17518253.2018.1547925
36. Pai, S., Sridevi, H., Varadavenkatesan, T., Vinayagam, R., Selvaraj, R.: Photocatalytic zinc oxide nanoparticles synthesis using *Peltophorum pterocarpum* leaf extract and their characterization. Optik. **185**, 248–255 (2019). https://doi.org/10.1016/j.ijleo.2019.03.101
37. Abdelbaky, A.S., Abd El-Mageed, T.A., Babalghith, A.O., Selim, S., Mohamed, A.M.H.A.: Green synthesis and characterization of ZnO nanoparticles using *Pelargonium odoratissimum* (L.) aqueous leaf extract and their antioxidant antibacterial and anti-infammatory activities. Antioxidants. **11**, 1444 (2022). https://doi.org/10.3390/antiox11081444
38. Sedefoglu, N.: Characterization and photocatalytic activity of ZnO nanoparticles by green synthesis method. Optik- Int. J. Light Electron. Opt. **288**, 171217 (2023). https://doi.org/10.1016/j.ijleo.2023.171217
39. Takcı, D.K., Sumengen Ozdenefe, M., Genc, S.: Green synthesis of silver nanoparticles with an antibacterial activity using *Salvia officinalis* aqueous extract. J. Cryst. Growth. **614**, 127239 (2023). https://doi.org/10.1016/j.jcrysgro.2023.127239
40. Narath, S., Koroth, S.K., Shankar, S.S., George, B., Mutta, V., Wacławek, S., ˇCerník, M., Padil, V.V.T., Varma, R.S.: *Cinnamomum tamala* leaf extract stabilized zinc oxide nanoparticles: A promising photocatalyst for methylene blue degradation. Nanomaterials. **11**(6), 1558 (2021). https://doi.org/10.3390/nano11061558
41. Faye, G., Jebessa, T., Wubalem, T.: Biosynthesis, characterisation and antimicrobial activity of zinc oxide and nickel doped zinc oxide nanoparticles using *Euphorbia abyssinica* bark extract.

IET Nanobiotechnol. **16**, 25–32 (2022). https://doi.org/10.1049/nbt2.12072
42. Zhang, G., Shen, X., Yang, Y.: Facile synthesis of monodisperse porous ZnO spheres by a soluble starch-assisted method and their photocatalytic activity. J. Phys. Chem. C. **115**, 7145–7152 (2011). https://doi.org/10.1021/jp110256s
43. Yang, X., Cao, X., Chen, C., Liao, L., Yuan, S., Huang, S.: Green synthesis of zinc oxide nanoparticles using aqueous extracts of *Hibiscus cannabinus* L.: Wastewater purification and antibacterial activity. Separations. **10**, 466 (2023). https://doi.org/10.3390/separations10090466
44. Awwad, A.M., Amer, M.W., Salem, N.M., Abdeen, A.O.: Green synthesis of zinc oxide nanoparticles (ZnO-NPs) using *Ailanthus altissima* fruit extracts and antibacterial activity. Chem. Int. **6**, 151–159 (2020). https://doi.org/10.5281/zenodo.3559520
45. Iqbal, J., Abbasi, B.A., Yaseen, T., Zahra, S.A., Shahbaz, A., Shah, S.A., Uddin, S., Ma, X., Raouf, B., Kanwal, S., Amin, W., Mahmood, T., El–Serehy, H.A., Ahmad, P.: Green synthesis of zinc oxide nanoparticles using *Elaeagnus angustifolia* L. leaf extracts and their multiple in vitro biological applications. Sci. Rep. **11**, 20988 (2021). https://doi.org/10.1038/s41598-021-99839-z
46. Ahmad, I., Alshahrani, M.Y., Wahab, S., Al-Harbi, A.I., Nisar, N., Alraey, Y., Alqahtani, A., Mir, M.A., Irfan, S., Saeed, M.: Zinc oxide nanoparticle: An efective antibacterial agent against pathogenic bacterial isolates. J. King Saud Univ-Sci. **34**(5), 102110 (2022). https://doi.org/10.1016/j.jksus.2022.102110
47. Vo, N.T.T., Do, M.Q., Van Pham, V.: Green chemistry synthesis and *Escherichia coli* antibacterial activity of silver and zinc oxide nanoparticles. J. Aust Ceram. Soc. **59**, 1205–1212 (2023). https://doi.org/10.1007/s41779-023-00926-3
48. Murali, M., Kalegowda, N., Gowtham, H.G., Ansari, M.A., Alomary, M.N., Alghamdi, S., Shilpa, N., Singh, S.B., Thriveni, M.C., Aiyaz, M., Angaswamy, N., Lakshmidevi, N., Adil, S.F., Hatshan, M.R., Amruthesh, K.N.: Plant-mediated zinc oxide nanoparticles: Advances in the new millennium towards understanding their therapeutic role in biomedical applications. Pharmaceutics. **13**(10), 1662 (2021). https://doi.org/10.3390/pharmaceutics13101662
49. Soltanian, S., Sheikhbahaei, M., Mohamadi, N., Pabarja, A., Abadi, M.F.S., Tahroudi, M.H.M.: Biosynthesis of zinc oxide nanoparticles using *Hertia Intermedia* and evaluation of its cytotoxic and antimicrobial activities. BioNanoScience. **11**, 245–255 (2021). https://doi.org/10.1007/s12668-020-00816-z
50. Mandal, A.K., Katuwal, S., Tettey, F., Gupta, A., Bhattarai, S., Jaisi, S., Bhandari, D.P., Shah, A.K., Bhattarai, N., Parajuli, N.: Current research on zinc oxide nanoparticles: Synthesis, characterization, and biomedical applications. Nanomaterials. **12**(17), 3066 (2022). https://doi.org/10.3390/nano12173066